Chem. Senses 29: 61–73, 2004 DOI: 10.1093/chemse/bjh006

Voltage-gated Inward Currents of Morphologically Identified Cells of the Frog Taste Disc

Takeshi Suwabe[1] and Yasuyuki Kitada[2]

[1]Department of Operative Dentistry and Endodontics, School of Dentistry, Iwate Medical University, Morioka 020-8505, Japan and [2]Department of Oral Physiology, School of Dentistry, Iwate Medical University, Morioka 020-8505, Japan

Correspondence to be sent to: Yasuyuki Kitada, Department of Oral Physiology, School of Dentistry, Iwate Medical University, Morioka 020-8505, Japan. e-mail: ykita@iwate-med.ac.jp

Abstract

We used the patch clamp technique to record from taste cells in vertical slices of the bullfrog (*Rana catesbeiana*) taste disc. Cell types were identified by staining with Lucifer yellow in a pipette after recording their electrophysiological properties. Cells could be divided into the following three groups: type Ib (wing) cells with sheet-like apical processes, type II (rod) cells with single thick rod-like apical processes and type III (rod) cells with thin rod-like apical processes. No dye-coupling was seen either between cells of the same type or between cells of different types. We focused on the voltage-gated inward currents of the three types of cells. Type Ib and type II cells exhibited tetrodotoxin (TTX)-sensitive voltage-gated Na^+ currents. Surprisingly, type III cells showed TTX-resistant voltage-gated Na^+ currents and exhibited a lack of TTX-sensitive Na^+ currents. TTX-resistant voltage-gated Na^+ currents in taste cells are reported for the first time here. The time constant for the inactivating portion of the voltage-gated inward Na^+ currents of type III cells was much larger than that of type Ib and type II cells. Therefore, slow inactivation of inward Na^+ currents characterizes type III cells. Amplitudes of the maximum peak inward currents of type III cells were smaller than those of type Ib and type II cells. However, the density (pA/pF) of the maximum peak inward currents of type III cells was much higher than that of type Ib cells and close to that of type II cells. No evidence of the presence of voltage-gated Ca^{2+} channels in frog taste cells has been presented up to now. In this study, voltage-gated Ba^{2+} currents were observed in type III cells but not in type Ib and type II cells when the bath solution was a standard Ba^{2+} solution containing 25 mM Ba^{2+}. Voltage-gated Ba^{2+} currents were blocked by addition of 2 mM $CoCl_2$ to the standard Ba^{2+} solution, suggesting that type III cells possess the voltage-gated Ca^{2+} channels and they do classical (calcium-influx) synaptic transmission. It appears that type III cells are taste receptor cells.

Key words: chemical transmission, frog, taste cell, TTX-resistant Na^+ current, type III cell, voltage-gated Ca^{2+} current

Introduction

In vertebrates, taste cells are found in clusters, known as taste buds, in the lingual epithelium. Taste cells can be divided into two major classes: elongated (type I, type II, type III) cells, which have processes extending into the taste pore, and ovoid basal (type IV) cells, which lie at the bottom of the taste bud without extending processes to the pore (for reviews, see Roper, 1989; Lindemann, 1996). Unlike mammalian taste buds with small apical pores, the frog taste organ (fungiform papilla) lacks a true pore and is disc-shaped. The frog taste discs contain diverse types of cells with different morphologies, but they contain all of the main morphotypes of taste cells that exist in vertebrates. On the basis of the structural features of taste cells, Osculati and Sbarbati (Osculati and Sbarbati, 1995) suggested that there were four major types (type I, type II, type III and type IV) of cells in the frog taste disc. Mucous (type Ia) cells have large cuboidal cell bodies in the surface layer of the taste disc and correspond to type I cells in the mammalian taste bud. Wing (type Ib) cells possess sheet-like processes that protrude between the mucous cells onto the surface. Rod cells are spindle-shaped cells with rod-like apical processes. They are subdivided into two groups: cells with thick apical processes (type II cells) and cells with thin apical processes (type III cells). Merkel-like basal (type IV) cells are located at the periphery of the taste disc and radiate with long processes into the center of the bottom of the taste disc. The above morphological observation was made using an electron microscope and partial serial reconstruction. Very recently, the morphology of viable taste discs of the frog was investigated using multi-photon microscopy (Li and

Lindemann, 2003). Fluorescent dye-loaded cells were clearly visualized in three dimensions, and the results of observation of the morphology of cell types using the new technique of multi-photon microscopy confirmed the results of observation in a previous study using classical electron microscopy (Osculati and Sbarbati, 1995). Osculati and Sbarbati (Osculati and Sbarbati, 1995) found synaptic-like contacts with afferent axons in type III cells, suggesting that type III cells are taste receptor cells. Type II cells contact with afferent axons but they lack granules and vesicles in a presynaptic position. Therefore, it is unclear whether type II cells are taste receptor cells. Type Ib cells lack any obvious contacts with afferent axons.

The patch-clamp technique has been used to investigate the membrane properties of taste cells isolated from taste buds by the use of proteolytic enzymes. Since rod cells and wing cells isolated from the frog taste disc retain their morphology after isolation, they can be readily identified. However, it is difficult to distinguish the subtypes (type II and type III) of isolated rod cells. Hence, we use the terms wing cells and rod cells for cells isolated from the frog taste disc. Like many elongated taste cells in vertebrates, rod cells isolated from frog taste discs have been reported to be electrically excitable. Isolated wing cells are also electrically excitable. Both rod cells (Avenet and Lindemann, 1987a) and wing cells (Miyamoto *et al.*, 1991; Bigiani *et al.*, 1998) possess voltage-gated Na^+ currents that are sensitive to tetrodotoxin (TTX) and voltage-gated K^+ currents. However, no evidence has so far been obtained for the presence of voltage-gated Ca^{2+} currents in frog taste disc cells (wing cells: Miyamoto *et al.*, 1991; Bigiani *et al.*, 1998; rod cells: Avenet and Lindemann, 1987a). Whole cell patch clamp recordings have recently been obtained in cells in slices of the frog taste disc without the use of proteolytic enzymes and cell isolation (Takeuchi *et al.*, 2001). In the preparation used by Takeuchi *et al.* (2001), the cellular organization of the taste disc was preserved. Takeuchi *et al.* (2001) identified four types (type Ia, type Ib, type II and type III) of cells in slices of the frog taste disc by staining with Lucifer yellow. Thus, we use the terms type Ia, type Ib, type II and type III cells for cells identified in a slice preparation. They showed that type Ia cells were electrically non-excitable and that type Ib, type II and type III cells displayed transient TTX-sensitive inward Na^+ currents and sustained outward K^+ currents in response to depolarization. Although Takeuchi *et al.* (Takeuchi *et al.*, 2001) reported the presence of voltage-gated currents in type III cells, little is known about the membrane properties of type III cells. It is important to investigate the membrane properties of type III cells, because type III cells have synaptic-like junctions with nerve terminals and are thought to be taste receptor cells (Osculati and Sbarbati, 1995). In the present study, we used a slice preparation of the frog taste disc. The use of whole cell patch clamp recording combined with cell identification using Lucifer yellow enabled us to identify distinct subpopulations of taste cells (type Ib, type II and type III cells) based on their electrophysiological properties. The present study focused on voltage-gated inward currents of type Ib, type II and type III cells, and the properties of these cell types were compared. We confirmed that type Ib and type II cells possess voltage-gated Na^+ currents that are sensitive to TTX and lack voltage-gated Ca^{2+} currents, as was reported for isolated wing cells and rod cells (Avenet and Lindemann, 1987a; Miyamoto *et al.*, 1991; Bigiani *et al.*, 1998). However, we report here that voltage-gated Na^+ currents that are resistant to TTX and voltage-gated Ca^{2+} currents are present in type III cells. This is the first report of the presence of TTX-resistant voltage-gated Na^+ currents in vertebrate taste cells and voltage-gated Ca^{2+} currents in frog taste cells.

Materials and methods

Preparation

Bullfrogs (*Rana catesbeiana*), weighing 200–400 g, were anesthetized with urethane (3 g/kg body wt). The experiments were performed in accordance with the Guidelines for Animal Experiments at Iwate Medical University. The tongues were removed from the animals. The fungiform papillae were dissected out from isolated tongues. Each fungiform papilla was cut vertically into ~100 μm slices with a fine scalpel under a binocular dissecting microscope. Slices were transferred into a recording chamber and fixed to the bottom of the recording chamber with the cut surface facing upward. The bottom of the recording chamber was previously treated with Cell-Tak (BD Biosciences, Bedford, MA) to improve adherence of the slices to the glass slide.

Recording

The recording chamber was placed on the stage of a microscope (BX50WI, Olympus, Tokyo, Japan) equipped with Nomarsky optics and a ×40 water-immersion objective. Lucifer yellow CH (Sigma, St Louis, MO) was added to the pipette solution. Cells were filled with Lucifer yellow during whole-cell recording, and they could be identified at the end of experiments. Fluorescent images of cells filled with Lucifer yellow were obtained using a fluorescent system (BX-FLA, Olympus) and photographed with a cooled CCD camera (DP-50, Olympus). Data of the fluorescent images were saved on a computer. Patch pipettes were made from borosilicate glass capillaries (WPI, Sarasota, FL) using a horizontal puller (P-97, Sutter, Novato, CA). When filled with the intracellular solution, the patch pipette resistance was 7–12 MΩ. Whole cell currents were measured at room temperature using a patch-clamp amplifier (EPC 8, HEKA electronik, Lambrecht, Germany). Signals were low-pass-filtered at 3 kHz, recorded, and analyzed using a computer equipped with an ITC-16 data acquisition interface (INSTRUTECH, Port Washington, NY) and PULSE and PULSE FIT software (HEKA electronik). IGOR software

(WaveMetrics, Lake Oswego, OR) was also used for analysis of the experimental data.

Solutions

Our standard bath solution was an amphibian physiological solution (APS) containing (concentrations in mM) 110 NaCl, 2 KCl, 2 $CaCl_2$, 1 $MgCl_2$, 20 glucose, 10 HEPES, buffered to pH 7.2 with NaOH. In some experiments, TTX (SANKYO Co., Tokyo, Japan) was dissolved in standard APS. The bath solution used for investigation of voltage-gated Ca^{2+} currents (standard $BaCl_2$ solution) contained (in mM) 25 $BaCl_2$, 80 tetraethylammonium chloride (TEACl), 0.001 TTX, 20 glucose, 10 HEPES, buffered to pH 7.2 with TEAOH. Two pipette solutions were used: one solution (standard KCl solution) contained (in mM) 105 KCl, 2 $MgCl_2$, 5 EGTA, 10 HEPES, buffered to pH 7.2 with KOH, and the other solution (standard CsCl solution) contained (in mM) 105 CsCl, 2 $MgCl_2$, 5 EGTA, 10 HEPES, buffered to pH 7.2 with CsOH.

Results

Cell types

Figure 1 shows a photomicrograph of the frog taste disc in vertical cross section. Mucous (type Ia) cells occupy the superficial layer (*a* in Figure 1) of the taste disc. Cell bodies of type Ib, type II and type III cells are all located in the intermediate layer (*b* in Figure 1) of the taste disc, but the location of cell bodies of type Ib cells in the intermediate layer is above the locations of type II and type III cells (Osculati and Sbarbati, 1995). Patch pipettes can be positioned in the intermediate layer under a microscope. Injection of Lucifer yellow enabled identification of taste cell types in a slice preparation after recording their electrophysiological properties.

Figure 2 shows examples of three type cells filled with Lucifer yellow. A type Ib cell had one sheet-like apical process reaching the free surface of the taste disc and one basal process that reached the base of the taste disc (Figure 2A). A type II cell had a spindle- or ovoid-shaped cell body with one rod-like apical process (Figure 2B). A type III cell had an ovoid- or spherical-shaped cell body with thinner rod-like apical processes (Figure 2C) than the apical processes of a type II cell. The single apical process of type III cell was tortuous, sometimes bifurcated (Figure 2C) or trifurcated. Some type III cells had furcated basal processes or several basal processes. Since the basal processes of type III cells ramified and have a variable shape in relation to the position of the cell body, the shape of basal processes of type III cell could not be shown in photographs satisfactory.

In the present study, 34 type Ib cells, 40 type II cells and 48 type III cells were identified by Lucifer yellow staining combined with electrophysiological recording. We could not observe any dye-coupling between cells of the same type or between cells of different types.

Passive membrane properties

Resting potentials were measured under a current clamp condition. APS was used as a bath solution and standard KCl solution was used as a pipette solution. The values of resting potential in type Ib, type II and type III cells were –59.1 ± 2.5 mV (mean ± SEM, $n = 6$), –56.3 ± 2.3 mV ($n = 6$) and –63.8 ± 4.0 mV ($n = 8$), respectively. The resting potentials in these cells were not significantly different (*t*-test, $P > 0.05$). Input resistances were measured by applying a 20 mV hyperpolarizing step pulse followed by a 20 mV depolarizing step pulse from a holding potential of –80 mV. The values of input resistance in type Ib, type II and type III cells were 3.3 ± 0.8 GΩ (mean ± SEM; $n = 10$), 9.9 ± 2.9 GΩ ($n = 10$) and 7.4 ± 1.8 GΩ ($n = 13$), respectively. Input resistance of type Ib cells was significantly smaller than those of type II and type III cells (*t*-test, $P < 0.01$). Cell membrane capacitance was measured at a holding potential of –80 mV. The values of cell membrane capacitance in type Ib, type II and

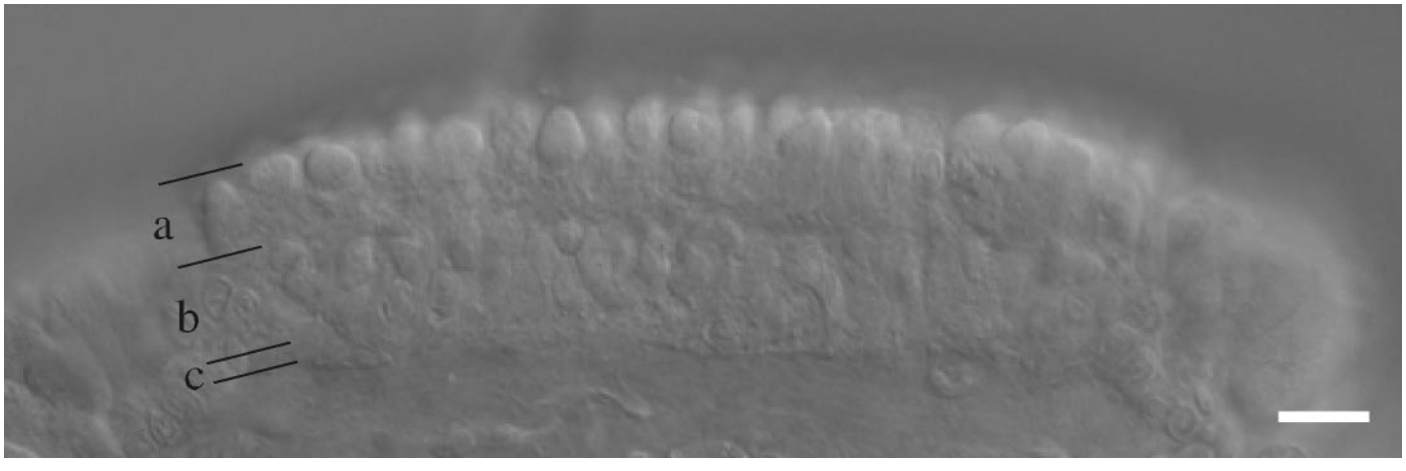

Figure 1 Photomicrograph of a slice preparation viewed with Nomarsky optics. Scale bar, 20 μm. a, the superficial layer; b, the intermediate layer; c, the basal layer.

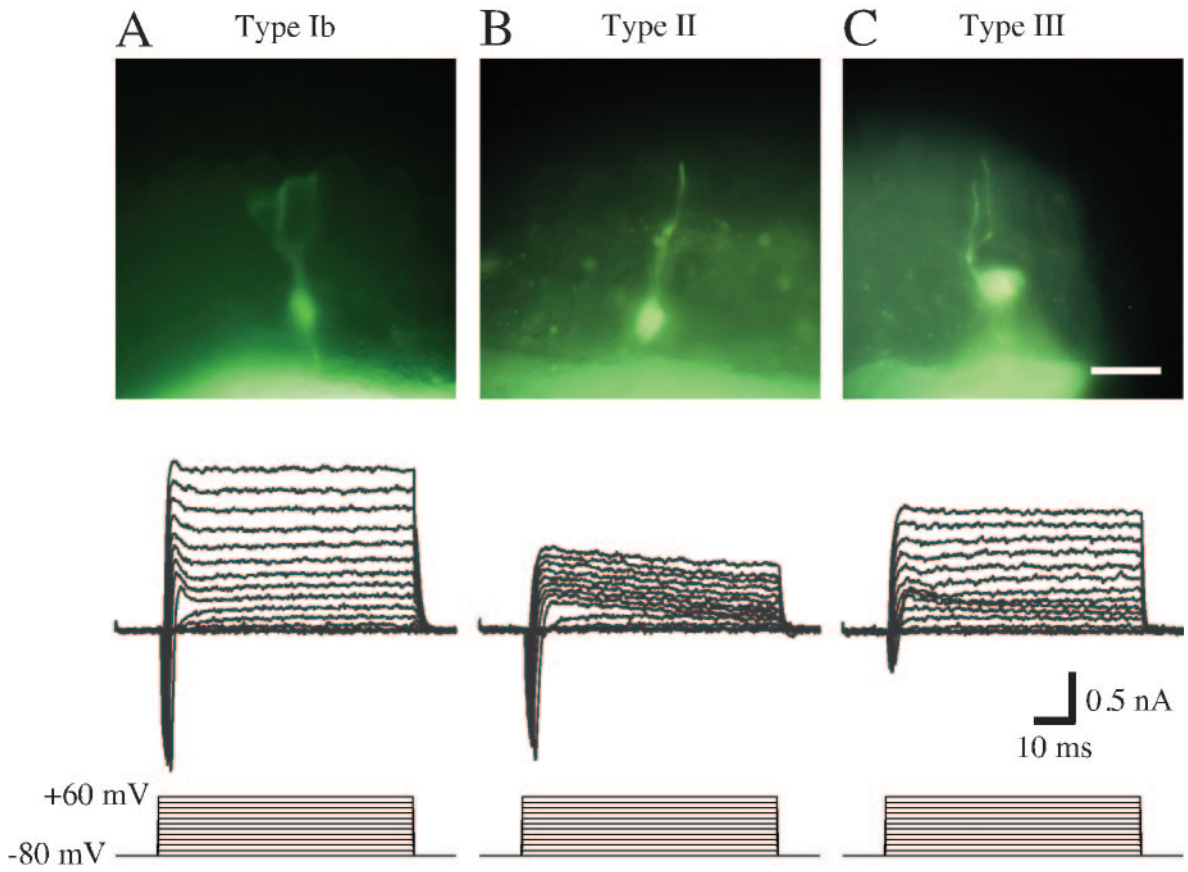

Figure 2 Three types of cells stained with Lucifer yellow and their whole-cell currents. **(A)** A type Ib cell. **(B)** A type II cell. **(C)** A type III cell. Scale bar, 20 μm. Inward and outward currents elicited by a series of depolarizing pulses between –70 and +60 mV, in 10 mV increments, from a holding potential of –80 mV. Each recording was obtained from the cell shown in the upper photomicrogragh. Bath solution was APS. The pipette solution was standard 105 mM KCl.

type III cells were 20.6 ± 1.5 pF (mean ± SEM; n = 10), 10.6 ± 1.5 pF (n = 12) and 4.3 ± 0.3 pF (n = 16), respectively. Cell membrane capacitance was significantly larger in type Ib cells than in type II and type III cells (t-test, $P < 0.01$).

Whole cell currents under voltage clamp

Voltage-gated ion currents in type Ib, type II and type III cells were recorded by application of depolarizing pulses from a holding potential of –80 mV. With APS in the bath and standard KCl solution in the pipette, the application of depolarizing pulses elicited transient inward currents and sustained outward currents in the three types of cells (Figure 2, bottom). Although Bigiani *et al.* (1998) reported that some isolated rod cells did not show any detectable transient inward currents, all three types of cells tested in slice preparations displayed transient inward currents.

Voltage-gated Na^+ currents

It has been reported that substitution of CsCl for KCl in the pipette eliminated the outward currents from the three types of cells (Takeuchi *et al.*, 2001). This implies that outward currents from the three types of cells are K^+ currents. In the present study, we focused on the inward currents. In subsequent experiments, the properties of inward currents were investigated with the pipette containing CsCl.

So far, voltage-gated Na^+ currents have been reported to be sensitive to TTX in isolated wing cells (Miyamoto *et al.*, 1991; Bigiani *et al.*, 1998) and rod cells (Avenet and Lindemann, 1987a), and in type Ib, type II and type III cells in slice preparations (Takeuchi *et al.*, 2001). Figure 3 shows the sensitivities of voltage-gated Na^+ currents to TTX. The transient inward currents recorded from a type Ib cell (Figure 3A) and a type II cell (Figure 3B) were blocked by addition of 1 μM TTX to APS. This effect was completely reversible. Surprisingly, 1 μM TTX in the bath solution did not block the transient inward currents recorded from a type III cell (Figure 3C). When sodium ions were replaced with *N*-methyl-D-glucamine (NMDG) ions in the bath, the inward currents recorded from a type III cell disappeared (see the third traces in Figure 3C). The results indicate that the inward currents in the three types of cells are carried through the voltage-gated Na^+ channels. The effects of various concentrations of TTX on the peak inward Na^+ currents of three types of cells are presented in Figure 4A.

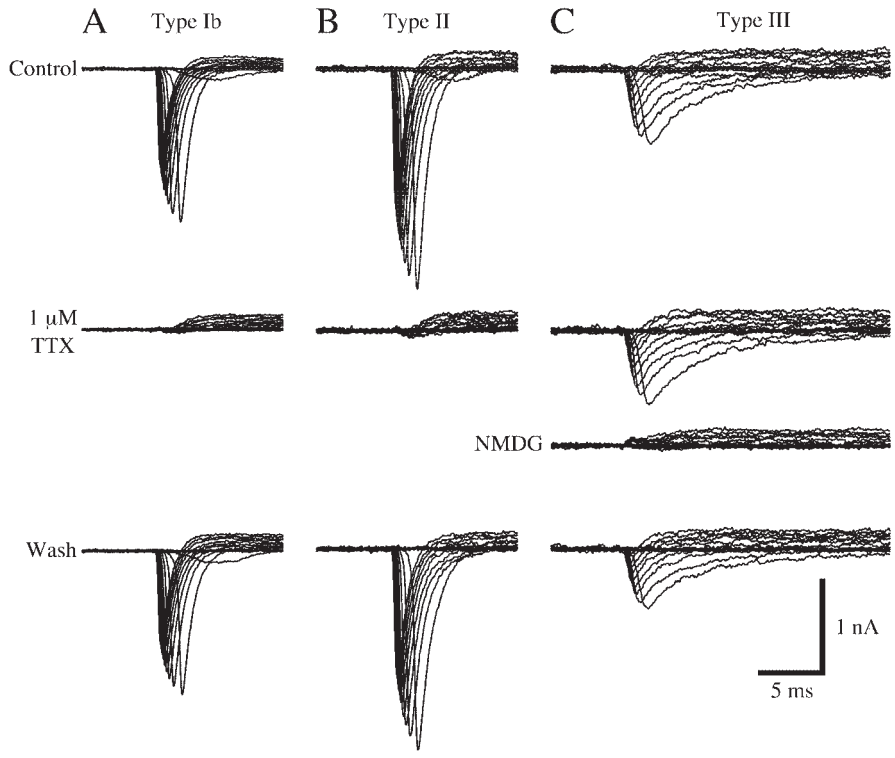

Figure 3 Sensitivity of voltage-gated Na^+ currents to TTX. Transient inward currents elicited by a series of depolarizing pulses between –70 and +60 mV, in 10 mV increments, from a holding potential of –80 mV. Pipette solution was standard 105 mM CsCl. **(A)** A type Ib cell. **(B)** A type II cell. **(C)** A type III cell. The transient inward currents recorded from a type Ib cell and a type II cell were completely blocked by 1 μM TTX added to APS. Addition of 1 μM TTX to APS did not eliminate the transient inward currents recorded from a type III cell, and the inward currents disappeared when sodium ions in the bath solution were replaced with NMDG ions.

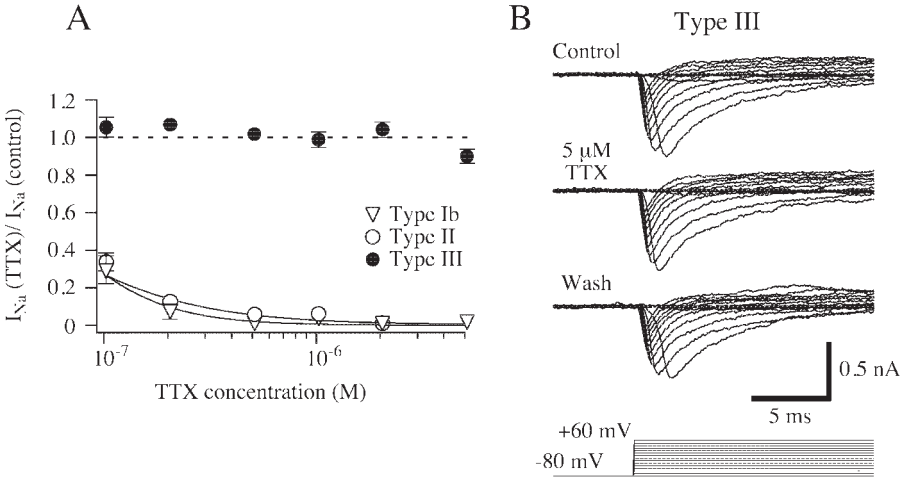

Figure 4 The effects of various concentrations of TTX on the peak inward Na^+ currents of three types of cells. **(A)** The maximum peak inward Na^+ currents (I_{Na}) with TTX were normalized with respect to that without TTX (control) and plotted against the concentration of TTX. The maximum peak inward Na^+ currents were obtained by a series of depolarizing pulses between –70 and +60 mV, in 10 mV increments, from a holding potential of –80 mV. Pipette solution was standard 105 mM CsCl. Each point represents mean ± SEM (bars). Type Ib cells (n = 3–4 cells). Type II cells (n = 3–6). Type III cells (n = 3–10). **(B)** Voltage-gated inward currents recorded from a type III cell are presented before, during and after application of 5 μM TTX. Voltage-clamp protocol: holding potential, –80 mV; depolarizing pulses in 10 mV increments from –70 to +60 mV. Bath solution, APS; pipette solution, standard 105 mM CsCl.

The inward Na^+ currents of type Ib and type II cells were almost completely eliminated by TTX in concentrations >0.5 μM. In type III cells, however, TTX at 0.1–5 μM did not affect the transient inward currents. Figure 4B shows that voltage-gated Na^+ currents recorded from a type III cell were not affected even during application of a high concen-

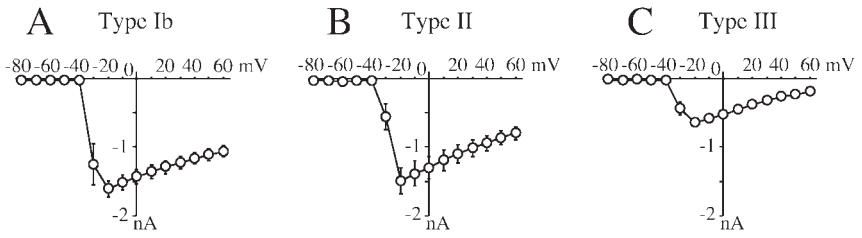

Figure 5 Current–voltage relationship of peak inward Na^+ currents in the three types of cells. **(A)** Type Ib cells (n = 9). **(B)** Type II cells (n = 10). **(C)** Type III cells (n = 14). Peak inward currents obtained by a series of depolarizing pulses between –70 and +60 mV, in 10 mV increments, from a holding potential of –80 mV, as a function of pulse voltage. Each point represents mean ± SEM (bars). Bath solution, APS; pipette solution, standard 105 mM CsCl.

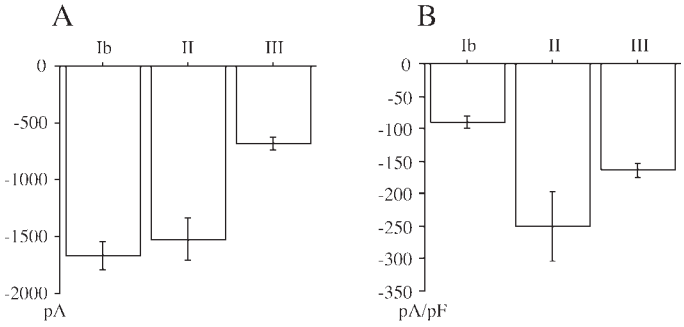

Figure 6 Maximum peak inward Na^+ currents and density of the maximum peak inward Na^+ current in the three types of cells. **(A)** Maximum values of voltage-gated Na^+ current measured at approximately –20 mV from a holding potential of –80 mV. **(B)** Magnitude of maximum peak inward current normalized to the membrane area expressed as membrane capacitance. The histograms represent mean values ± SEM (bars) from nine type Ib cells, 10 type II cells and 14 type III cells. Bath solution, APS; pipette solution, standard 105 mM CsCl.

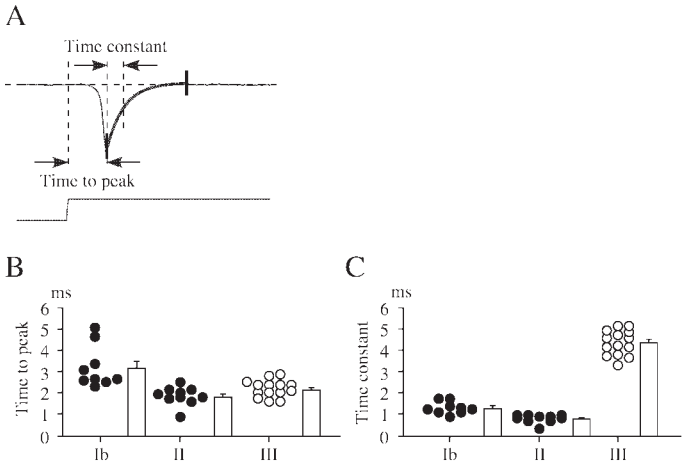

Figure 7 Activation and inactivation time courses for sodium currents in the three types of cells. **(A)** An example of time course of an inward current with maximum peak current in response to depolarization from a holding potential of –80 mV. The decay time course was fitted with a single exponential function. Individual values of the time to peak **(B)** and the time constant for the inactivating time course of sodium currents **(C)** in nine type Ib cells, 10 type II cells and 14 type III cells are shown. Columns represent mean values ± SEM (bars) in the three types of cells. When the sensitivity of voltage-gated Na^+ currents to 1 μM TTX was examined, all nine type Ib cells and all 10 type II cells were TTX-sensitive (filled symbols), and all 14 type III cells were TTX-resistant (open symbols).

tration of TTX (5 μM). These results indicate that voltage-gated Na^+ channels of type Ib and type II cells are TTX-sensitive and that voltage-gated Na^+ channels of type III cells are TTX-resistant.

The transient inward currents in the three types of cells were activated by depolarization exceeding –40 mV from a holding potential of –80 mV and peaked at approximately –20 mV (Figure 5). Peak amplitudes of the inward currents in type Ib, type II and type III cells were –1666 ± 124 pA (mean ± SEM; n = 9), –1523 ± 190 pA (n = 10) and –680 ± 50 pA (n = 14), respectively (Figure 6A). The peak amplitude was significantly smaller in type III cells than in type Ib and type II cells (t-test, $P < 0.001$). However, after normalizing the peak amplitude to the membrane capacitance, statistical analysis revealed that the current density was significantly smaller in type Ib cells than in type II and type III cells (t-test, $P < 0.05$) (Figure 6B).

As shown in Figure 3, the time course of inactivation of the voltage-gated Na^+ current recorded from a type III cell was much slower than those from other types of cells. The time course of an inward Na^+ current shown in Figure 7A illustrates the time to peak for the activating portion and the time constant for the inactivating portion in an inward Na^+ current. The decay of the current was fitted with a single exponential function. As shown in Figure 7B, the values of the time to peak were significantly longer in type Ib cells than those in other types of cells (t-test, $P < 0.001$). The decay time constants of inward Na^+ currents in individual cells are shown in Figure 7C. The mean values of the time constants in type Ib, type II and type III cells were 1.3 ± 0.1 ms (mean ± SEM; n = 9), 0.8 ± 0.1 ms (n = 10) and 4.4 ± 0.2 ms (n = 14), respectively. The differences among the three types of cells were statistically significant (t-test, $P < 0.001$). The order for the slow inactivation of the voltage-gated Na^+ channel was type III >> type Ib > type II. It is clear that slow inactivation of the voltage-gated Na^+ channel characterizes type III cells. Therefore, we were able to distinguish type III cells from type Ib and type II cells by time courses of

inactivation of inward currents. Cells showing resistance to TTX exhibited slow inactivation of inward currents (Figure 7C).

Voltage dependence of inward Na^+ current inactivation was investigated using a typical two-pulse protocol (prepulse and test pulse). The inward current (I), as obtained with a test pulse to –10 mV from different holding potentials (at which cells were held for 1 s), was normalized to I_{max}, measured at a holding potential of –100 mV. The plot of I/I_{max} as a function of holding potential resulted in a sigmoid curve (Figure 8) that could be fitted by the equation

$$I/I_{max} = 1/\{1 + \exp[(V - V_{0.5})/k]\}$$

where $V_{0.5}$ is the membrane potential at which the current showed half-inactivation, and k is the slope. The values for half-inactivation voltage in type Ib, type II and type III cells were –41.2, –44.0 and –39.8 mV, respectively, and the slopes in type Ib, type II and type III cells were 7.3, 6.7 and 5.4 mV, respectively (pooled data from six cells in each cell type). Bigiani *et al.* (1998) reported that the value for half-inactivation voltage in isolated wing cells was –70.7 mV, which was more negative than that of type Ib obtained here. The difference in results between the present study and the previous study is due to methodological variables for duration of the prepulse. In their experiments, the prepulse was applied to the cell for long periods of time (10 s). It has been shown that half-inactivation voltage in isolated rat taste cells was more negative in long duration of the prepulse than in short duration (Herness and Sun, 1995).

Voltage-gated Ca^{2+} currents

Ba^{2+} is known to pass through Ca^{2+} channels as well as or better than Ca^{2+} (Bean, 1989). To test for the presence of voltage-gated Ca^{2+} currents in the three types of cells, we used standard $BaCl_2$ solution as a perfusion solution and standard CsCl solution as a pipette solution. Since the standard $BaCl_2$ solution contained Ba^{2+}, TTX and TEA^+ in the absence of Na^+, voltage-gated Na^+ and K^+ currents could not appear. Hence, the presence of voltage-gated Ba^{2+} currents would be obvious. We could not detect voltage-gated Ba^{2+} currents in type Ib and type II cells even in this experimental condition (Figure 9A,B). In type III cells, however, sustained inward currents were clearly detected in the standard $BaCl_2$ solution (the third traces in Figure 9C and the middle traces in Figure 10A). No voltage-gated inward currents were elicited when 25 mM $BaCl_2$ was replaced with 35 mM NMDG (the second traces in Figure

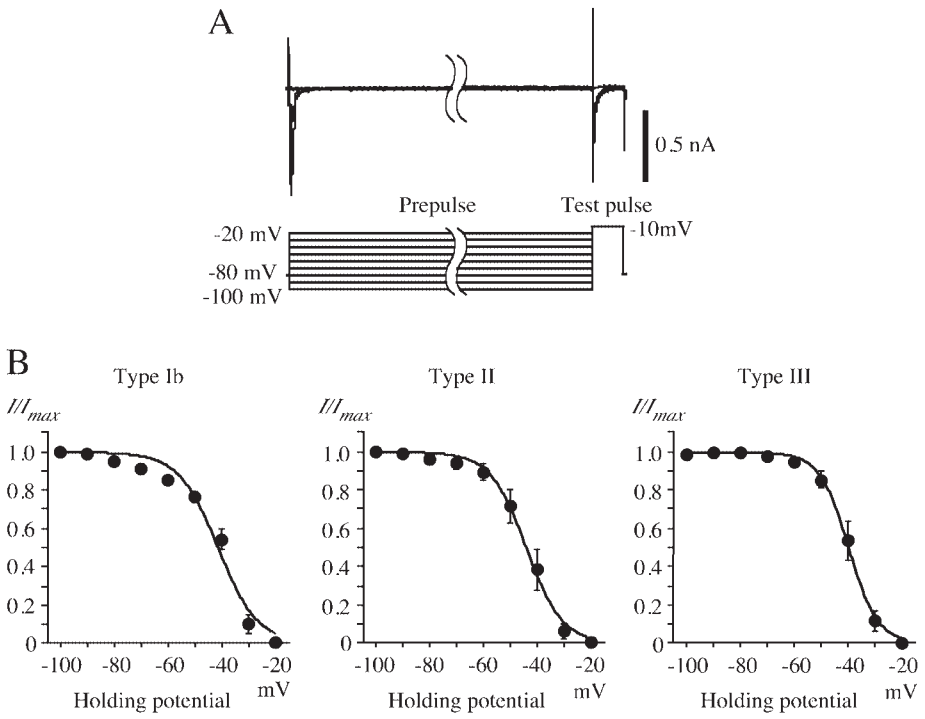

Figure 8 Inactivation of voltage-gated Na^+ currents in the three types of cells. **(A)** Inward Na^+ currents were elicited by application of depolarizing pulse (test pulse) to –10 mV after holding the membrane potential (prepulse) of various amplitudes (–100 to –20 mV) for 1 s **(B)** Peak currents (I) during a depolarizing pulse to –10 mV were normalized with respect to that obtained at a holding potential of –100 mV (I_{max}) and plotted as a function of holding potential. Bath solution, APS; pipette solution, standard 105 mM CsCl. Each point represents mean ± SEM (bars) for type Ib cells (n = 6), type II cells (n = 6) and type III cells (n = 6). In each type of cell, the data points were fitted by a sigmoid curve. Half-maximal voltages for type Ib, type II and type III cells were –41.2, –44.0 and –39.8 mV, respectively, and the values of the slope were 7.3, 6.7 and 5.4 mV, respectively.

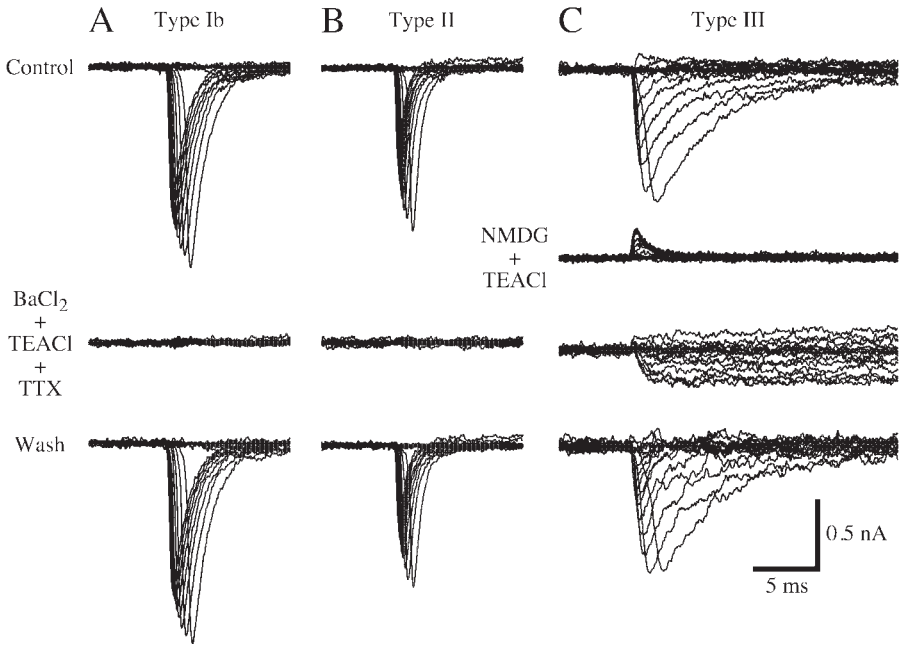

Figure 9 Test for presence for voltage-dependent Ca^{2+} currents in the three types of cells. Transient inward currents were elicited by a series of depolarizing pulses between –70 and +60 mV, in 10 mV increments, from a holding potential of –80 mV. Pipette solution was standard 105 mM CsCl. **(A)** A type Ib cell. **(B)** A type II cell. **(C)** A type III cell. (A, B) Absence of voltage-dependent Ca^{2+} currents in type Ib cell and type II cell. Bath solution was APS (first traces). Transient inward Na^+ currents disappeared when the bath solution was standard $BaCl_2$ solution of 25 mM $BaCl_2$, 80 mM TEACl, 1 μM TTX, 10 mM HEPES (pH 7.2) (second traces). Transient inward Na^+ currents reappeared when the bath solution was changed to APS again (third traces). (C) Presence of voltage-dependent Ca^{2+} current in type III cell. Bath solution was APS (first traces). Transient inward Na^+ currents disappeared when bath solution was Na-free, 35 mM NMDG, 80 mM TEACl, 10 mM HEPES (pH 7.2) (second traces). Voltage-gated sustained inward currents appeared when the bath solution was standard $BaCl_2$ solution (third traces). Transient inward Na^+ currents reappeared when the bath solution was changed to APS again (fourth traces).

9C). Addition of 2 mM $CoCl_2$, a known Ca^{2+} channel blocker, to the standard $BaCl_2$ solution blocked the voltage-gated Ba^{2+} currents. Current-voltage relationships for the peak inward currents with and without 2 mM $CoCl_2$ are shown in Figure 10B. The peak inward currents with $CoCl_2$ were then subtracted from those without $CoCl_2$ to obtain the Co^{2+}-sensitive currents (Ba^{2+} currents). Ba^{2+} currents were activated around –40 mV and reached a peak at 0 mV. Peak amplitude of the Ba^{2+} currents was –164.8 pA at 0 mV. We concluded that voltage-gated Ca^{2+} channels are present in type III cells. However, the voltage-gated Ba^{2+} currents that appeared in the standard $BaCl_2$ solution rapidly waned with time after recording (rundown of Ba^{2+} currents). Furthermore, voltage-gated Ca^{2+} currents could not be detected when $BaCl_2$ was replaced with $CaCl_2$ (data not shown).

It should be noted that sustained inward currents independent of voltage appeared in type III cells when APS was replaced with the standard $BaCl_2$ solution (the middle traces in Figure 10A). The inward current measured at –80 mV was –17.6 ± 6.5 pA (mean ± SEM, n = 9). Since the inward current disappeared when the bath solution was changed to APS again (the right traces in Figure 10A), the inward component independent of voltage is not due to a leak current. Similar inward currents were also observed in bath solutions containing 25 mM Ca^{2+} (data not shown). The inward component was not reduced by 2 mM $CoCl_2$. Type III cells did not display rundown of the inward current independent of voltage. Inward currents could not be observed in type Ib and type II cells.

Contribution of Na^+ currents to action potentials in response to current injections

To investigate the contribution of Na^+ currents to action potential, cells were made to generate action potentials by depolarizing current pulses under current-clamp conditions. Type Ib, type II and type III cells generated action potentials when the bath perfusion was APS (Figure 11). In the presence of 1 μM TTX, type Ib and type II cells did not generate action potentials, but type III cells did generate action potentials. When the sodium ions in the bath solution were replaced with NMDG ions, type III cells no longer generated action potential (Figure 11C). These results indicate that TTX-sensitive Na^+ currents contribute to the generation of action potentials in type Ib and type II cells and that TTX-resistant Na^+ currents contribute to the generation of action potentials in type III cells.

Discussion

Membrane properties of frog taste organ cells have been extensively studied by using the patch-clamp technique to

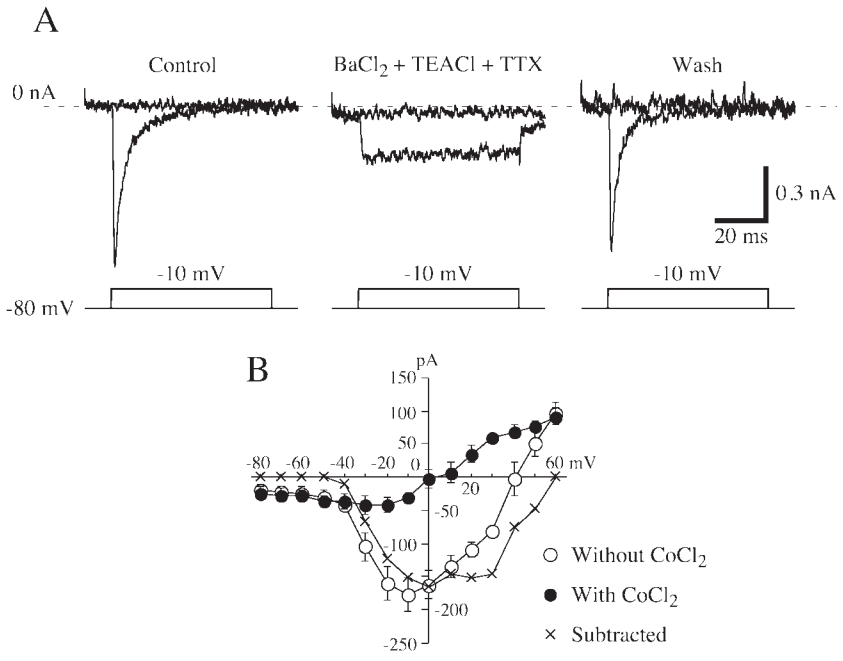

Figure 10 Voltage-gated Ba^{2+} currents in type III cells. **(A)** Left and right: bath solution, APS. The inward Na^{+} currents in response to a depolarizing pulse to –10 mV from a holding potential of –80 mV. Middle: bath solution, standard $BaCl_2$ solution. Inward Ba^{2+} current in response to a depolarizing pulse to –10 mV from a holding potential of –80 mV. Pipette solution was standard 105 mM CsCl. Dotted line represents 0 nA. Note that sustained inward currents (approximately –20 pA) appeared only in standard $BaCl_2$ solution (middle). **(B)** Peak current–voltage relationship of voltage-gated currents in standard $BaCl_2$ solution with and without 2 mM $CoCl_2$. Inward currents were elicited by a series of depolarizing pulses between –70 and +60 mV, in 10 mV increments, from a holding potential of –80 mV. The Co^{2+}-sensitive current (the Ba^{2+} current) was determined by subtracting the curve obtained under full block of Co^{2+} from the curve (without Co^{2+}). Each point represents mean ± SEM (bars). Open circle symbols, $n = 9$; filled circle symbols, $n = 5$.

isolated wing cells and rod cells (for review, see Lindemann, 1996). Wing cells can be readily identified by the presence of sheet-like apical process, whereas a rod-like apical process characterizes rod cells. On the basis of their structural features (Osculati and Sbarbati, 1995), rod cells have been divided into two subpopulations: cells having a pear-shaped body with one thick straight apical process (type II cells) and cells having a spherical cell body with thin apical processes and with several basal processes stemming directly from the cell body (type III cells). In isolated rod cells, however, it has not been possible to divide into the two subpopulations: type II and type III cells. It is probable that isolated type III cells with thin apical processes might lose their morphological features due to damage inflicted during the isolation procedure. Therefore, it is likely that information on membrane properties of type III cells can not be obtained from isolated rod cells. Takeuchi *et al.* (2001) used the patch clamp technique to record from cells in vertical slices of the frog taste disc. They morphologically identified type Ia (mucous), type Ib, type II and type III cells by staining the cells with Lucifer yellow after recording their electrophysiological properties and showed that Ia cells lacked voltage-gated currents but that type Ib, type II and type III cells had voltage-gated inward Na^{+} currents and outward K^{+} currents. Our results obtained by using slice preparations confirmed and extended their findings by showing characteristics of voltage-gated inward currents of type Ib, type II and type III cells.

Passive membrane properties

A number of investigators have shown dye-coupling between neighboring cells in vertebrate taste buds (for reviews, see Lindemann, 1996; Bigiani, 2002), including those in frogs (Sata *et al.*, 1992). Dye-coupled cells have a much higher membrane capacitance than that obtained from non-coupled receptor cells (Bigiani and Roper, 1993). In the present study, we failed to find dye-coupling between neighboring cells in slice preparations of the frog taste disc. This result is in agreement with that reported previously (Takeuchi *et al.*, 2001). Hence, the present data were obtained from single cells.

The values of resting potential, input resistance and cell membrane capacitance in the three types of cells were measured. The resting membrane potential values in the three types of cells were almost identical, around –60 mV. Cell membrane capacitance was much larger in type Ib cells than in type II and type III cells. Input resistance was smaller in type Ib cells than in the other cell types. The findings for cell membrane capacitance and input resistance are consistent with differences between membrane surface areas of the apical processes in type Ib and other types of cells (type II and type III cells). The values of resting potential, input

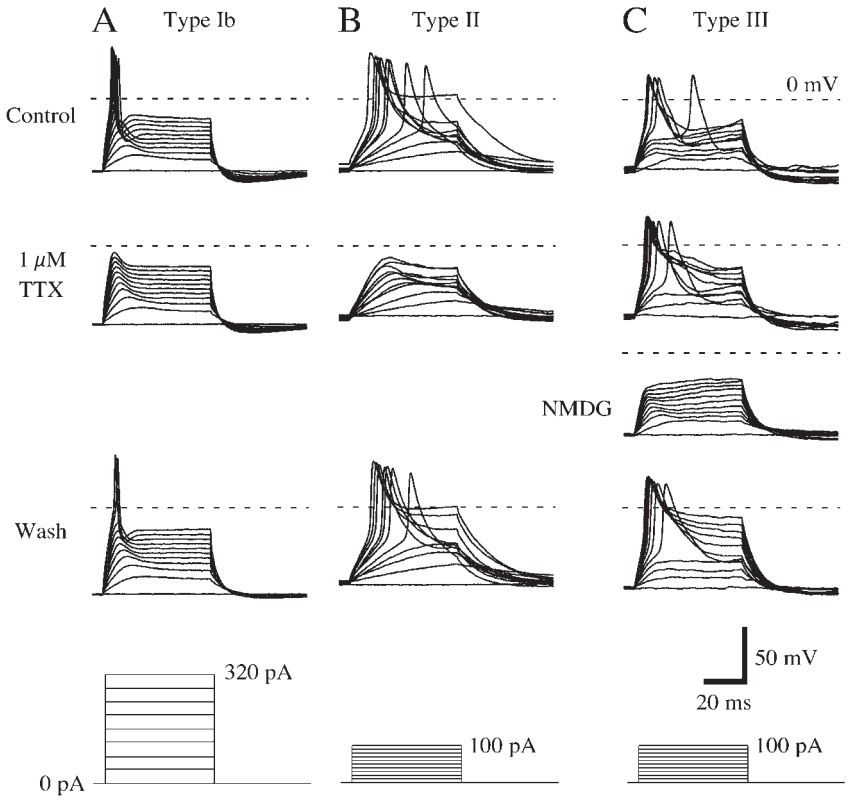

Figure 11 Contribution of sodium currents to action potential in the three types of cells. Pipette solution was standard 105 mM KCl. **(A)** A type Ib cell (control, resting potential = –62.2 mV). **(B)** A type II cell (control, resting potential = –63.3 mV). **(C)** A type III cell (control, resting potential = –63.4 mV). (A) and (B) Action potentials recorded from a type Ib cell and a type II cell under current-clamp conditions. In control conditions (bath solution: APS), action potentials were elicited by a series of depolarizing pulses between 40 and 320 pA in 40 pA increments in a type Ib cell and between 10 and 100 pA in 10 pA increments in a type II cell (first traces). Addition of 1 μM TTX to APS completely eliminated the action potentials (second traces). In a voltage-clamp configuration, the inward Na^+ currents were completely abolished by 1 μM TTX (data not shown). The action potentials reappeared when the bath solution was changed to APS again (third traces). (C) Action potentials recorded from a type III cell under current-clamp conditions. In control conditions (bath solution: APS), action potentials were elicited by a series of depolarizing pulses between 10 and 100 pA in 10 pA increments (first traces). Addition of 1 μM TTX to APS did not eliminate the action potentials (second traces). In a voltage-clamp configuration, the inward Na^+ currents were not abolished by 1 μM TTX (data not shown). When the sodium ions in the bath solution were exchanged with NMDG ions, current injections failed to elicit an action potential (third traces). The action potentials reappeared when the bath solution was changed to APS again (fourth traces).

resistance and cell membrane capacitance in type Ib cells in slice preparations were similar to those obtained from isolated wing cells (Bigiani *et al.*, 1998), suggesting that the membrane electrical properties of isolated wing cells were preserved during the dissociation procedure. For type II and type III cells, the mean values of 9.9 GΩ in type II and of 7.4 GΩ in type III cells obtained in the present study were higher than the mean value of 4.1 GΩ obtained in isolated rod cells (Bigiani *et al.*, 1998). The use of a proteolytic enzyme during the dissociation procedure may alter the electrophysiological membrane properties of isolated rod cells. Bigiani *et al.* (1998) reported that some rod cells did not show any detectable voltage-gated Na^+ currents and possessed K^+ currents only. We could not find any cells (type Ib, type II and type III cells) lacking voltage-gated Na^+ currents in our slice preparations. Okada *et al.* (2001) reported that almost all isolated rod cells of frogs displayed transient inward currents. In that study, the mean value for the input resistance of isolated rod cells was 7.0 GΩ . This value in isolated rod cells was close to the mean value of 9.9 GΩ in type II and of 7.4 GΩ in type III obtained here. It is possible that membrane properties of cells are not always altered by cell dissociation.

TTX-sensitive and TTX-resistant Na^+ currents

Voltage-gated inward Na^+ currents have been found in many vertebrate taste cells (for review, see Lindemann, 1996; Bigiani, 2002). They are sensitive to TTX. In frogs, TTX-sensitive voltage-gated Na^+ currents have been reported in isolated wing cells (Miyamoto *et al.*, 1991; Bigiani *et al.*, 1998) and rod cells (Avenet and Lindemann, 1987a) and in type Ib, type II and type III cells of slice preparations (Takeuchi *et al.*, 2001). We also showed that type Ib and type II cells had TTX-sensitive voltage-gated Na^+ currents. However, it is surprising that all type III cells investigated in the present study had TTX-resistant voltage-gated

Na^+ currents and lacked TTX-sensitive Na^+ currents. Although electrical signals of excitable cells in vertebrates are fundamentally dependent on TTX-sensitive voltage-gated Na^+ channels, TTX-resistant Na^+ currents have been found in a variety of animals and tissues, such as mammalian dorsal root ganglia, petrosal ganglia, nodose ganglia and small-diameter peripheral neurons (for review, see Yoshida, 1994). It has been shown that the activation and inactivation process of TTX-resistant Na^+ channels is slower than that of TTX-sensitive Na^+ channels (for review, see Yoshida, 1994). In the present study, the time constant for the inactivating portion of the TTX-resistant Na^+ currents was much larger than that of TTX-sensitive Na^+ currents (Figure 7). Hence, slow inactivation of inward Na^+ currents characterizes type III cells.

Our data are very different from those obtained by Takeuchi *et al.* (2001), who reported that voltage-gated Na^+ currents of type III cells were sensitive to TTX. It is probable that the difference in results between the present study and the previous study is due to methodological variables for identification of cell types. In the study by Takeuchi *et al.* (2001), cell types were identified only by their morphological features. The numbers of cells used in experiments to examine the sensitivity to TTX were not stated in their paper. In our study, the time course of the inactivating portion of voltage-gated Na^+ currents, combined with cell type identification using Lucifer yellow staining, enabled us to identify type II and type III cells. All type III cells identified by both their morphological features and slow inactivation of inward Na^+ currents were insensitive to TTX, and other types of cells were sensitive to TTX (Figure 7).

Although sensitivity to TTX in voltage-gated Na^+ currents of type III cells differs from that of type Ib and type II cells, some properties of voltage-gated Na^+ currents in the three types of cells are identical. As shown in Figure 5, in the three types of cells, Na^+ current was activated at –40 mV and reached a peak at –20 mV (Figure 5). The kinetics of Na^+ channel inactivation determined by the use of a two-pulse protocol are shown in Figure 8. Half-inactivation potentials for the three types of cells were almost the same, between –40 and –44 mV. However, amplitudes of the maximum peak currents of type III cells were smaller than those of type Ib and type II cells (Figures 5 and 6A). This finding is consistent with that previously reported (Takeuchi *et al.*, 2001). From the characteristics of the small inward current of type III cells, Takeuchi *et al.* (2001) suggested that type III cells are immature cells, still in the midway stage of development, because expression of voltage-gated inward currents is incomplete in immature cells (Mackay-Sim *et al.*, 1996). However, the density (pA/pF) of the maximum peak inward currents of type III cells was much higher than that of type Ib cells and close to that of type II cells (Figure 6B). Therefore, it is likely that type III cells are mature cells.

Voltage-gated Ca^{2+} currents and chemical transmission

By using the whole-cell voltage clamp technique, voltage-gated Ca^{2+} channels have been found in taste cells of amphibians (for review, see Bigiani, 2002), rats (Behe *et al.*, 1990) and mice (Medler *et al.*, 2003). However, there is no evidence of the presence of voltage-gated Ca^{2+} channels in isolated frog wing cells (Miyamoto *et al.*, 1991; Bigiani *et al.*, 1998) or rod cells (Avenet and Lindemann, 1987a). In the present study, we observed voltage-gated sustained Ba^{2+} inward currents in type III cells in standard $BaCl_2$ solution. The voltage-gated inward currents were blocked by addition of 2 mM Co^{2+} to the standard $BaCl_2$ solution. We concluded that voltage-gated Ca^{2+} channels are present in type III cells. Classical chemical synapses are usually associated with voltage-gated Ca^{2+} channels. Since type III cells are able to generate action potentials (Figure 11) and they form synaptic-like contacts with afferent axons (Osculati and Sbarbati, 1995), it appears that type III cells are taste receptor cells. However, it is unclear whether taste stimulation of type III cells in the frog produce depolarization that reach threshold and evoke action potentials. It has been demonstrated that amphibian taste cells are able to generate action potentials in response to a chemical stimulus ($CaCl_2$) applied to the mucosal surface (Avenet and Lindemann, 1987b).

Sustained inward currents independent of voltage appeared only in type III cells when APS was replaced with the standard $BaCl_2$ solution that contained 25 mM $BaCl_2$ and 80 mM TEACl. It has been shown that various salts applied to the tongue produce neural response in the frog glossopharyngeal nerve (Kusano, 1960; Nomura and Sakada, 1965; Kitada, 1978; Kitada, 1994). In pilot work, we observed that application of 25 mM $BaCl_2$ alone, 80 mM TEACl alone or the standard $BaCl_2$ ($CaCl_2$) solution with and without 2 mM $CoCl_2$ used in this study to the tongue is effective for producing neural responses. Therefore, it is probable that the standard $BaCl_2$ solution activates a cationic conductance in type III cells as a taste stimulus and induce an inward current. Additional studies are needed to clarify the characteristics of the inward current.

We show that type Ib and type II cells are able to generate action potentials but they lack voltage-gated Ca^{2+} currents. Anatomical studies reported that type Ib cells lack any obvious contacts with afferent axons (Osculati and Sbarbati, 1995). Based on electrophysiological studies, Bigiani *et al.* (1998) pointed out that the presence of ion channels in wing (type Ib) cells might be suggestive of a role in controlling the microenvironment inside the taste organs or the functioning of chemosensory cells or both. However, it is unknown how type Ib cells participate in the taste transduction. Since type II cells contact with afferent axons (Osculati and Sbarbati, 1995), it is possible that type II cells serve as taste receptors. The lack of voltage-gated Ca^{2+} currents in type II cells suggests that type II cells may not communicate with nervous system using conventional synapse. If type II cells

participate directly in taste transduction, the transmission from type II cells to afferent axons would be mediated by Ca^{2+} release from intracellular stores or Ca^{2+} influx through Ca^{2+}-permeable non-selective cation channels. In rat taste cells, denatonium, a bitter-tasting compound, induces Ca^{2+} release from intracellular stores (Akabas *et al.*, 1988). It has been proposed that bitter and sweet tastants might activate phosphodiesterase via gustducin, resulting in a reduction of cyclic nucleotide level in taste cells (Wong *et al.*, 1996). The reduction of cyclic nucleotide levels in taste cells resulted in activation of cyclic-nucleotide-suppressive conductance leading to Ca^{2+} influx through non-selective cation channels and cell depolarization (Kolesnikov and Margolskee, 1995). Saccharin activates cation conductance via inositol 1,4,5-trisphosphate production in a subset of isolated rod cells in the frog (Okada *et al.*, 2001).

Morpho-functional correlation for taste cells

The study to correlate electrophysiological properties with taste cell structural features was performed with isolated *Necturus* taste cells (McPheeters *et al.*, 1994). The taste cells investigated were identified after recording by electron microscope. In that study, dark (type I) cells had voltage-gated Na^+, K^+ and Ca^{2+} currents. Light (type II) cells were divided into two functional populations based upon electrophysiological criteria: cells with voltage-gated Na^+, K^+ and Ca^{2+} currents and cells with only voltage-gated outward K^+ currents. Very recently, morpho-functional correlation for isolated mammalian taste cells was reported (Medler *et al.*, 2003). Taste cell types isolated from mouse vallate and foliate papillae were identified by using antibodies to external epitopes. Antigen H-immunoreactive (-IR) (type I) cells, many antigen A-IR (type II) cells and all gustducin-expressing (type II) cells had small voltage-gated inward Na^+ and outward K^+ currents but no voltage-gated inward Ca^{2+} currents. In contrast, a subset of antigen A-IR (type II) cells and all neural cell adhesion molecules-IR (type III) cells had large voltage-gated Na^+, K^+ as well as voltage-gated inward Ca^{2+} currents. In frog taste cells, we showed that type I and type II cells had TTX-sensitive voltage-gated Na^+ currents, voltage-gated K^+ currents but no voltage-gated Ca^{2+} currents and that type III cells had TTX-resistant voltage-gated Na^+, voltage-gated K^+ and voltage-gated Ca^{2+} currents. The previous data and our data suggest that there is a good correlation between electrophysiological properties and cell morphotypes in vertebrate taste organs.

Acknowledgements

We thank Drs K. Okuda-Akabane and K. Narita for their critical comments on an earlier draft of the manuscript. We are grateful to Professor M. Kubota, School of Dentistry, Iwate Medical University, for his contributions to this study. This work was supported by a Grand-in-Aid for Scientific Research (no. 14571771) to Y. Kitada and High Performance Biomedical Materials Research from the Ministry of Education, Culture, Sports, Science and Technology, Japan.

References

Akabas, M.H., Dodd, J. and **Al-Awqati, Q.** (1988) *A bitter substance induces a rise in intracellular calcium in a subpopulation of rat taste cells*. Science, 242, 1047–1050.

Avenet, P. and **Lindemann, B.** (1987a) *Patch-clamp study of isolated taste receptor cells of the frog*. J. Membrane Biol., 97, 223–240.

Avenet, P. and **Lindemann, B.** (1987b) *Action potentials in epithelial taste receptor cells induced by mucosal calcium*. J. Membrane Biol., 95, 265–269.

Bean, B.P. (1989) *Classes of calcium channels in vertebrate cells.* Annu. Rev. Physiol., 51, 367–384.

Behe, P., DeSimone, J.A., Avenet, P. and **Lindemann, B.** (1990) *Membrane currents in taste cells of the rat fungiform papilla: evidence for two types of Ca currents and inhibition of K currents by saccharin*. J. Gen. Physiol., 96, 1061–1084.

Bigiani, A. (2002) *Electrophysiology of* Necturus *taste cells*. Prog. Neurobiol., 66, 123–159.

Bigiani, A. and **Roper, S.D.** (1993) *Identification of electrophysiologically distinct cell subpopulations in* Necturus *taste buds*. J. Gen. Physiol., 102, 143–170.

Bigiani, A., Sbarbati, A., Osculati, F. and **Pietra, P.** (1998) *Electrophysiological characterization of a putative supporting cell isolated from the frog taste disk*. J. Neurosci., 18, 5136–5150.

Herness, M.S. and **Sun, X.D.** (1995) *Voltage-dependent sodium currents recorded from dissociated rat taste cells*. J. Membrane Biol., 146, 73–84.

Kitada, Y. (1978) *Inhibitory effects of cations on the Ca^{2+} response of water fibers in the frog tongue*. Jpn. J. Physiol., 28, 413–422.

Kitada, Y. (1994) *The responses to choline ions induced by transition metal ions in single water fibers of the frog glossopharyngeal nerve*. Chem. Senses, 19, 627–640.

Kolesnikov, S.S. and **Margolskee, R.F.** (1995) *A cyclic-nucleotide-suppressible conductance activated by transducin in taste cells*. Nature, 376, 85–88.

Kusano, K. (1960) *Analysis of the single unit activity of gustatory receptors in the frog tongue*. Jpn. J. Physiol., 10, 620–633.

Li, J.H. and **Lindemann, B.** (2003) *Multi-photon microscopy of cell types in the viable taste disk of the frog*. Cell Tissue Res., 313, 11–27.

Lindemann, B. (1996) *Taste reception*. Physiol. Rev., 76, 719–766.

Mackay-Sim, A., Delay, R.J., Roper, S.D. and **Kinnamon, S.C.** (1996) *Development of voltage-dependent currents in taste receptor cells*. J. Comp. Neurol., 365, 278–288.

McPheeters, M., Barber, A.J., Kinnamon, S.C. and **Kinnamon, J.C.** (1994) *Electrophysiological and morphological properties of light and dark cells isolated from mudpuppy taste buds*. J. Comp. Neurol., 346, 601–612.

Medler, K.F., Margolskee, R.F. and **Kinnamon, S.C.** (2003) *Electrophysiological characterization of voltage-gated currents in defined taste cell types of mice*. J. Neurosci., 23, 2608–2617.

Miyamoto, T., Okada, Y. and **Sato, T.** (1991) *Voltage-gated membrane current of isolated bullfrog taste cells*. Zool. Sci., 8, 835–845.

Nomura, H. and **Sakada, S.** (1965) *On the 'water response' of frog's tongue*. Jpn. J. Physiol., 15, 433–443.

Okada, Y., Fujiyama, R., Miyamoto, T. and **Sato, T.** (2001) *Saccharin activates cation conductance via inositol 1,4,5-trisphosphate produc-*

tion in a subset of isolated rod taste cells in the frog. Eur. J. Neurosci., 13, 308–314.

Osculati, **F.** and **Sbarbati, A.** (1995) *The frog taste disc: a prototype of the vertebrate gustatory organ*. Prog. Neurobiol., 46, 351.

Roper, **S.D.** (1989) *The cell biology of vertebrates taste receptors*. Annu. Rev. Neurosci., 12, 329–353.

Sata, O., Okada, Y., Miyamoto, T. and **Sato, T.** (1992) *Dye-coupling among frog (*Rana catesbeiana*) taste disk cells*. Comp. Biochem. Physiol., 103A, 99–103.

Takeuchi, H., Tsunenari, T., Kurahashi, T. and **Kaneko, A.** (2001) *Physiology of morphologically identified cells of the bullfrog fungiform papilla*. Neuroreport, 12, 2957–2962.

Wong, G.T., Gannon, K.S. and **Margolskee, R.F.** (1996) *Transduction of bitter and sweet taste by gustducin.* Nature, 381, 796–800.

Yoshida, **S.** (1994) *Tetrodotoxin-resistant sodium channels*. Cell. Mol. Neurobiol., 14, 227–244.

Accepted November 17, 2003